In silico screening of GMQ-like compounds reveals guanabenz and sephin1 as new allosteric modulators of acid-sensing ion channel 3

Gerard Callejo, Luke A. Pattison, Jack C. Greenhalgh, Sampurna Chakrabarti, Evangelia Andreopoulou, James R. F. Hockley, Ewan St. John Smith* and Taufiq Rahman*.

Department of Pharmacology, University of Cambridge, Tennis Court Road, Cambridge CB2 1PD, UK

**Corresponding authors: Ewan St. John Smith, es336@cam.ac.uk and Taufiq Rahman, mtur2@cam.ac.uk.*

Keywords: acid-sensing ion channel, GMQ, Sephin1, nociception

Abstract

Acid-sensing ion channels (ASICs) are voltage-independent cation channels that detect decreases in extracellular pH. Dysregulation of ASICs underpins a number of pathologies. Of particular interest is ASIC3, which is recognised as the key sensor of acid-induced pain and is instrumental in the establishment of pain arising from inflammatory conditions, such as rheumatoid arthritis. Thus, the identification of new ASIC3 modulators and the mechanistic understanding of how these compounds modulate ASIC3 could be important for the development of new strategies to counteract the detrimental effects of dysregulated ASIC3 activity in inflammation. Here, we report the identification of novel ASIC3 modulators based on the ASIC3 specific agonist, 2-guanidine-4-methylquinazoline (GMQ). Through a GMQ-guided *in silico* screening of Food and Drug administration (FDA)-approved drugs, 5 compounds were selected and tested for their possible modulation of rat ASIC3 (rASIC3) using whole-cell patch-clamp electrophysiology. Of the chosen drugs, guanabenz, an α2-adrenoceptor agonist, produced similar effects to GMQ on rASIC3, activating the channel at neutral pH and potentiating its response to mild acidic stimuli. Sephin1, a guanabenz derivative that lacks α2-adrenoceptor activity, has been proposed to act as a selective inhibitor of a regulatory subunit of the stress-induced protein phosphatase 1 (PPP1R15A) with promising therapeutic potential for the treatment of multiple sclerosis. However, we found that like guanabenz, sephin1 activates rASIC3 at neutral pH and potentiates its response to acidic stimulation, i.e. sephin1 is a novel modulator of rASIC3. Furthermore, docking experiments showed that, like GMQ, guanabenz and sephin1 likely interact with the nonproton ligand-sensing domain of rASIC3. Overall, these data demonstrate the utility of computational analysis for identifying novel ASIC3 modulators, which can be validated with electrophysiological analysis and may lead to the development of better compounds for targeting ASIC3 in the treatment of inflammatory conditions.

Introduction

Extracellular protons modulate the activity of a wide range of ion channels and receptors, which activate sensory neurons involved in nociception and the development of pain [1]. One key group of proton sensors is the acid-sensing ion channel (ASIC) family, these voltage-independent, ligand-gated cation channels are activated by extracellular protons [2–4] and belong to the amiloride-sensitive epithelial sodium channel/degenerin (ENaC/DEG) ion channel family [5,6]. In mammals, four genes (*accn1-4*) encode for at least 6 different ASIC subunits (ASIC1a, ASIC1b, ASIC2a, ASIC2b, ASIC3, ASIC4), which can assemble into homo- and heterotrimeric channels displaying different pH sensitivity, current kinetics and pharmacology [7–9]. ASICs are widely expressed in the central and peripheral nervous systems [2,10] and are implicated in a range of physiological and pathological processes including nociception, mechanosensation and learning/memory [2,5,11–13]. The involvement of ASICs in such a plethora of physiological and pathological roles makes them attractive pharmacological targets for drug development and a variety of agents have been identified that act as agonists/antagonists for these channels with differing levels of selectivity [14]. Of the ASIC subunits, there is good evidence that ASIC3 is a critical acid sensor involved in acid-induced pain. ASIC3 homomers are the most sensitive to decreases in extracellular pH [7], in response to which they produce a biphasic inward current composed of a large, rapidly desensitizing transient current, followed by a smaller, non-desensitizing sustained window current (resulting from an overlap between pH-dependent activation and inactivation curves) that lasts for the duration of the acidic stimulus [15,16]. Although protons appear to be the main endogenous activators of ASICs, other molecules that modulate ASIC function have been discovered. For instance, endogenous molecules such as arachidonic acid and anandamide [17], serotonin [18], dynorphins [19] and lactate [20] all enhance ASIC3 currents in response to acidic stimulation. In addition, 2-guanidine-4-methylquinazoline (GMQ) [21], agmatine [22] and lysophosphatidylcholine [23] can activate ASIC3 at neutral pH by increasing the sustained, window current. Moreover, a range of toxins isolated from animal venoms also modulate ASIC function [24]. Among them, APETx2, a toxin isolated from the sea anemone *Anthopleura elegantissima*, inhibits the transient

component of ASIC3 activation in response to an acidic stimulus (pH 4) without affecting its sustained component [25] and it has been used to establish the role of ASIC3 in a number of physiological and pathological processes, including inflammatory pain [26]. Nevertheless, the relationship between ASIC3, pain and inflammation is complex. Several histological studies, as well as those employing pharmacological ASIC3 modulation, have determined an involvement of ASIC3 in pain elicited in deep tissues such as joints, muscle and the viscera [27–33]. However, further studies using ASIC3-deficient mice have suggested a more limited role in pain [34], as well as a proposed dual role of ASIC3 in arthritis where lack of ASIC3 ameliorates pain, but increases inflammatory processes in the arthritic joint [35]. A possible explanation of these controversial results could be that inflammatory processes are sometimes [36], but not always [37], accompanied by acidosis. Nevertheless, the complex and controversial role of ASIC3 in some inflammatory processes requires the development of better pharmacological tools to dissect its precise function in such conditions. To this end, in the present study we hypothesised that we could employ GMQ as a query structure in a ligand-based *in silico* screening of FDA-approved drugs to identify novel ASIC3 modulators. From the results of the screening, we selected five different compounds with chemical and structural similarities to GMQ. From all drugs tested, guanabenz (GBZ), an antihypertensive drug, caused an enhancement of acid-induced rASIC3 activation and, like GMQ, it also activated the channel at neutral pH. Given that GBZ is an agonist of α2-adrenoceptors [38], and with the goal of identify a more selective ASIC3 modulator, we evaluated the effect of sephin1, a GBZ derivative that has no adrenoceptor activity that may be of use in protein misfolding diseases such as multiple sclerosis [39]. Similarly to GBZ and GMQ, sephin1 was activated rASIC3 at neutral pH and potentiated its activation in response to a mild acidosis. In summary, we demonstrate that ligand-based *in silico* approaches can be useful to identify novel small molecule modulators of ASIC3. Indeed, we have identified, from a library of FDA-approved drugs that have been proven safe for their use in humans, novel ASIC3 modulators that enhance rASIC3 activity, proving that this approach can serve to identify potential new ASICs modulating drugs that could be useful for treatment of inflammatory disorders.

Materials and Methods

Ligand-based screening

The 3D structure of GMQ was obtained from pubchem (pubchem CID: 345657) and was subsequently energy-minimised using MMFF94 force field implemented in OpenBabel version 2.4.0 [40]. Using the energy-minimised GMQ structure as a 3D query, Rapid Overlay of Chemical Structures (ROCS) (version 3.2.2.2, OpenEye Scientific Software, Santa Fe, NM) [41] was used to screen a conformer library generated from eDrug3D database [42] that contains 1884 different molecular structures including structures of enantiomers and of active metabolites of FDA-approved drugs. The conformer library was generated using Omega 3.0.1.2 (OpenEye Scientific Software) [43]. For each alignment, ROCS compares 3D shape and chemical similarity and returns a Tanimoto Combo (TC) score, ranging from 0 to 2, that includes a Shape Tanimoto (maximum 1) and Colour Tanimoto (scaled colour score, maximum 1) [44]. Following manual inspection of the top 150 hits ranked by the TC score, a subset of drugs was selected for experimental testing. Molecular field-based alignment [45] of drug structures with GMQ was performed using Forge (v 10.4.2; Cresset®, Litlington, Cambridgeshire, UK).

Chinese hamster ovary cell culture and transfection

Chinese hamster ovary (CHO) cells (Sigma, passage 6 to 20) were chosen for this study due to the absence of endogenous ASIC-like currents [46] and were grown using standard procedures in the following medium: Ham's F-12 Nutrient Mixture (Life Technologies), 10 % fetal bovine serum (Sigma), 1 % Penicillin/Streptomycin (100 U/ml, Life Technologies). 24-hours before transfecting cells, 35 mm dishes (Fisher) were coated with 100 µg/ml poly-L-lysine (Sigma) and cells from a 70-80% confluent flask were trypsinised, resuspended in 5 ml CHO medium and a volume was taken to seed cells at a 1:10 dilution (2 ml/dish). For transfections, an EGFP expression vector was used to enable identification of transfected cells and DNA was transfected at a ratio of 20:1 (rASIC3:GFP), using 1.5 µg rASIC3 DNA and 0.075 µg EGFP DNA; the transfection reagent Lipofectamine LTX (Life Technologies) was used according to the manufacturer's protocol.

144

145 ## Whole-cell electrophysiology

146 Whole-cell patch clamp recordings from CHO cells were performed at room
147 temperature 24-hours after transfection. For all the experiments, the intracellular
148 solution contained (in mM) 110 KCl, 10 NaCl, 1 $MgCl_2$, 1 EGTA, 10 HEPES, 2
149 Na_2ATP, 0.5 Na_2GTP in MilliQ water; pH was set to pH 7.3 by adding KOH and
150 the osmolality was adjusted to 310-315 mOsm with sucrose. The extracellular
151 solution contained (in mM) 140 NaCl, 4 KCl, 2 $CaCl_2$, 1 $MgCl_2$, 10 HEPES, 4
152 Glucose in MilliQ water; osmolality was adjusted to 300-310 mOsm with sucrose
153 and pH was adjusted to 7.4 with NaOH. Patch pipettes were pulled from glass
154 capillaries (Hilgenberg) using a Model P-97, Flaming/Brown puller (Sutter
155 Instruments) and had a resistance of 4-8 MΩ. Data were acquired using an
156 EPC10 amplifier (HEKA) and Patchmaster software (HEKA) after suitable
157 resistance compensation. To measure the effect of the different selected
158 compounds on rASIC3 current amplitude and inactivation time constant the
159 following protocol was used. After 5 s of pH 7.4 solution, pH 6 or pH 7 was applied
160 for 5 s to determine the baseline rASIC3 response. Then, in the first group of
161 experiments, a second pH 6 application was performed after 10 s of pH 7.4 and
162 30 s of compound application to determine the effect of these compounds on
163 rASIC3. In the second group of experiments, after the initial pH 7 baseline rASIC3
164 response, compounds were applied at pH 7 after 30 s of pH 7.4 to measure the
165 effect of the selected compounds on pH 7 rASIC3 activation. Finally, a third 5 s
166 pH 6 or pH 7 application was performed after 30s of pH 7.4 solution to determine
167 reversibility of any possible effect of the compounds on the channel. For dose-
168 response recordings of sephin1 at neutral pH and pH 7, increasing concentrations
169 of sephin1 were applied for 10 s with a 30 s wash period with extracellular pH 7.4
170 solution between each application. For pH-response recordings, extracellular
171 solutions with a pH ranging from 7.4 to 5 with/without sephin1 were applied for
172 10 s with a 30 s wash period between applications. All compounds/acidic
173 solutions were applied to cells through a gravity-driven 12-barrel perfusion
174 system [47]. In all the experiments the holding potential was set at -60mV.

175

176 ## Molecular Docking

177 We used a homology model of rASIC3 (Uniprot accession: O35240) based on
178 the 1.9 Å crystal structure of chicken ASIC1 homotrimer (PDB id: 2QTS; [8]) as a
179 template. Detail of the model building was previously reported [48]. Selected
180 drugs were docked to the rASIC3 model using the Lamarckian genetic algorithm
181 (LGA) implemented in AutoDock 4.2.6 [49]. For all docking, an unbiased ("blind")
182 docking approach was used where the entire rASIC3 trimer was used for
183 generating the grid map in AutoGrid. Prior to docking, structures of all drugs
184 (obtained from PubChem) and the rASIC3 trimer were prepared using the
185 AutoDock Tools. Five independent docking runs were performed for each drug
186 and the pose associated with the highest reproducibility and lowest predicted free
187 energy of interaction (ΔG, kcal/mol) was considered as the final pose for each
188 drug. From the top-ranked poses of the docked drugs, the 2D ligand interaction
189 diagrams were generated using PoseView™ implemented in the ProteinsPlus
190 webserver (https://proteins.plus/). Open-Source PyMOL 1.8 (Schrodinger, LLC)
191 was used for all molecular representations.
192

193 ## Drugs

194 All the small molecules used in this study were purchased from Sigma except for
195 tizanidine (Tocris) and APETx2 (Smartox). Stock solutions were made at 100 mM
196 for tizanidine (in H_2O), guanabenz (EtOH), cycloguanil (DMSO) and sephin1
197 (DMSO), 50 mM for GMQ (DMSO) and brimonidine (H_2O), and 40 mM for
198 guanfacine (H_2O). For most experiments, compounds were diluted in pH 7.4 or
199 pH 7 extracellular solution at 500 μM, however, GMQ, guanabenz and sephin1
200 were diluted in extracellular pH 7.4 solution at 1 mM for one set of experiments.
201 An APETx2 stock solution was made at 100 μM and diluted at 1 μM in pH 7.4
202 extracellular solution.
203

204 ## Data analysis

205 Absolute peak amplitudes were measured by subtracting the peak amplitude
206 response from the 5-second mean baseline prior to stimulation. Peak amplitude
207 was then normalised by dividing the absolute peak amplitude by the capacitance
208 of the cell to obtain peak current density (pA/pF). The inactivation time constant
209 was measured with a single exponential equation using a built-in function of

210 Fitmaster. The sustained current to transient current ratio was calculated by
211 measuring the size of the sustained current (peak sustained response at the end
212 of the stimulus minus the 5-second mean baseline current) and dividing his value
213 by the peak amplitude current (I_{sus}/I_{peak} x 100). The analysis of ASIC3 current
214 amplitudes and kinetics was performed as previously reported [9]. Statistical
215 analysis was performed in GraphPad Prism using a paired t-test comparing the
216 baseline pH response (pA/pF) against the pH response after compound
217 application for each cell. Data were plotted as a percentage of the initial pH
218 response for each cell. Results are expressed as mean ± standard error of the
219 mean (SEM), unless otherwise stated. For dose-response curves, all
220 measurements were expressed as a percentage of the pH baseline peak current
221 value (pH 6 or pH 7). For pH-response curves, all measurements were
222 transformed to percent of the maximum peak current (I/Imax x 100). The EC_{50} for
223 both dose- and pH-response (pH_{50}) experiments were determined using a
224 standard Hill equation using GraphPad Prism. For the pH-response curve in the
225 presence of sephin1 a biphasic equation was used in GraphPad Prism. For the
226 analysis of pH-dependent effect of sephin1 on the rASIC3 sustained current a
227 Gaussian distribution equation was used in GraphPad Prism. All figures were
228 made using GraphPad Prism and Adobe Illustrator CS6.

Results

Ligand-based *in silico* screening of novel ASIC3 modulators

Using the energy-minimised 3D structure of GMQ as a query, we used ROCS to screen a conformer library of FDA-approved drugs (eDrug3D) [42]. ROCS aligns each conformer from the target chemical library against the query or bait structure and quantifies the overall similarity between the aligned ligands as the Tanimoto Combo (TC) score. The latter is the sum of the Shape Tanimoto and the Color Tanimoto (scaled colour score), which represent the measure of similarity in 3D shape and chemical properties between the aligned moieties, respectively [44]. Of the top 150 hits ranked by the TC score, we manually inspected each individual hit for the degrees of 3D shape overlap and chemical similarity with GMQ, paying particular attention to the presence of a guanidine (or similar) moiety. This finally led us to shortlist 5 drugs, namely tizanidine (TIZ), cycloguanil (CG), brimonidine (BRI), guanfacine (GF) and GBZ (Fig. 1A). Of these hits, GBZ and GF contain an explicit (i.e. free) guanidine group (shown in red in Fig.1B), whereas CG, BRI and TIZ have an 'implicit' (i.e. within a ring) guanidine moiety.

To assess how these drugs compare to GMQ in terms of overall surface electrostatics, they were aligned to the energy-minimised GMQ structure using the software Forge™ (Cresset, UK), which uses a proprietary molecular mechanics-based ('XED') forcefield to generate and compare molecular 'field points' between aligned molecules (Fig. 1B). These field points represent positions of maximum interaction of a molecule with its electrostatic, steric and hydrophobic surroundings and thus effectively provides a 'protein-centric' view of a ligand. Upon alignment, Forge produces a field similarity score that takes both volume and molecular field points into account and a field score >0.7 is often regarded as indicator of reasonably good electrostatic similarities between the query and the bait molecule [45]. GBZ both qualitatively and quantitatively has the highest field point similarity with GMQ; in decreasing order of similarity of molecular fields, compound similarity with GMQ was computed as: BRI > TIZ > GF > CG (Fig. 1B).

262 **Effect of selected drugs on acid-induced rASIC3 activation.**

263 The following set of experiments were conducted to determine if the selected
264 drugs modulate rASIC3 function. We performed whole-cell patch clamp
265 recordings in CHO cells co-transfected with rASIC3 and EGFP and evaluated the
266 effect of 30 s application of each drug (500 μM) on the rASIC3 response to pH 6.
267 In this series of experiments, we also evaluated the effect of GMQ and APETx2,
268 which were used as positive controls. As expected, in rASIC3-expressing CHO
269 cells, APETx2 (1μM) application did not activate the channel at neutral pH, but
270 produced a significant inhibition of transient (I_{Peak}, Fig. 2A-B, n = 10, paired t-test,
271 p = 0.0013) and sustained (I_{5s}, Fig. 2A, n = 10, paired t-test, p = 0.029) current
272 evoked by pH 6 (Table 1). However, the ratio I_{5s}/I_{Peak} was significantly increased
273 (Fig 2C and Table 1, n = 10, paired t-test, p = 0.036), indicating that the
274 predominant APETx2 inhibitory effect is exerted on the transient phase as
275 previously described [25]. In addition, APETx2 significantly inhibited the
276 inactivation time constant (Tau) of rASIC3 (Fig. 2D and Table 1, n = 10, paired t-
277 test, p = 0.0005). By contrast, GMQ generated a sustained inward current at pH
278 7.4 as reported previously [21], but did not significantly modulate channel current
279 amplitude or inactivation kinetics (Table 1).
280
281 Among the 5 drugs tested in these series of experiments (summarised in Table
282 1), with the exception of GBZ, none of them produced a significant change on
283 rASIC3 current amplitude or inactivation kinetics (Fig. 2B-D). Unlike all other
284 compounds tested, and in a similar fashion to GMQ, we observed that GBZ, a
285 drug currently used to treat hypertension, activated rASIC3 at neutral pH (Fig.
286 2A). However, unlike GMQ, pre-application of GBZ elicited a significant increase
287 in the transient and sustained components of the pH 6-induced rASIC3 current
288 (Fig. 2B and Table 1, I_{Peak}, n = 11, paired t-test, p = 0.0173; I_{5s}, n = 11, paired t-
289 test, p = 0.015). The stronger potentiating effect upon the sustained current
290 (403%) compared with the effect on the transient current (113%) produced a
291 significant increase in the I_{5s}/I_{Peak} ratio (Fig. 2C and Table 1, n = 11, paired t-test,
292 p = 0.016) and the inactivation time constant of the pH 6-induced rASIC3
293 response was significantly increased by GBZ (Fig. 2D and Table 1, n = 11, paired
294 t-test, p = 0.014).

295 **Effect of GBZ on rat ASIC3 response to mild acidosis.**

296 Millimolar concentrations of GMQ are required to activate rASIC3 channels at
297 neutral pH, but at micromolar concentrations, GMQ sensitises pH 7-induced
298 rASIC3 channel activation [21]. At neutral pH, even though both GMQ and GBZ
299 (1 mM), are capable of activating rASIC3, the activation of rASIC3 by GBZ is of
300 smaller magnitude compared to GMQ-induced rASIC3 activation (11 ± 1.6% for
301 GMQ vs 5 ± 1.1 for GBZ, Fig.3A and 3B). Given the structural and chemical
302 similarities between GMQ and GBZ (Fig. 1), we next tested the effect GBZ (500
303 μM) on pH 7-induced rASIC3 activation to determine if, like GMQ, it also
304 sensitises the pH 7 response of rASIC3. As expected, the application of GMQ
305 (500 μM) at pH 7 elicited a significant sensitisation of rASIC3 by increasing the
306 amplitude of both transient and sustained current components (I_{peak} pH 7: 50 ±
307 5.9 pA/pF vs I_{peak} pH 7 + GMQ: 203.4 ± 34.8 pA/pF, paired t-test, n = 9, p = 0.001;
308 I_{5s}: 13.3 ± 1.5 pA/pF vs 132.5 ± 25.4 pA/pF, paired t-test, n = 9, p = 0.0012, Fig.
309 3C and 3D), and also increased the I_{5s}/I_{peak} ratio (I_{5s}/I_{peak} pH 7: 26.8± 1.2 % vs
310 I_{5s}/I_{peak} pH 7 + GMQ: 63.7 ± 2 %, paired t-test, n = 9, p < 0.0001, Fig. 3D),
311 suggesting a stronger effect on the sustained component of rASIC3. Similarly,
312 GBZ (500 μM) potentiated the pH 7-induced rASIC3 activation (I_{peak} pH 7: 159.3
313 ± 36 pA/pF vs I_{peak} pH 7 + GBZ: 418.6 ± 103.5 pA/pF, paired t-test, n = 6, p =
314 0.038; I_{5s}: 52.3 ± 9.6 pA/pF vs 342.1 ± 82.6 pA/pF, paired t-test, n = 6, p = 0.012;
315 I_{5s}/I_{peak} pH 7: 35 ± 4.9 % vs I_{5s}/I_{peak} pH 7 + GBZ: 81.3 ± 3.2 %, paired t-test, n =
316 6, p = 0.012, Fig. 3B and 3D), suggesting a similar mechanism of rASIC3
317 modulation. However, as observed for the activation of rASIC3 at neutral pH, the
318 sensitising effect on the transient component of the pH 7-induced rASIC3
319 activation by GBZ was smaller than that elicited by GMQ, although the effect of
320 both molecules on the ratio I_{5s}/I_{peak} was of comparable magnitude (I_{peak} GMQ:
321 408.1 ± 44.9 % vs I_{peak} GBZ: 275.4 ± 25.3 %; I_{5s}/I_{peak} GMQ: 240.3 ± 9.1 % vs
322 I_{5s}/I_{peak} GBZ: 259.6 ± 42.5 %, Fig. 3D).

323

324 The carboxyl-carboxylate interaction pair formed by the residues E79 and E423
325 in the palm domain of rASIC3 has been implicated in GMQ binding and the cavity
326 where these two amino acids are localised has been named the 'nonproton ligand
327 sensor domain' because several 'nonproton' ASIC3 ligands such as GMQ,

328 agmatine and serotonin all bind this domain [18,21,22]. Although GBZ shares
329 certain structural and chemical properties with GMQ, including a guanidine
330 moiety (Fig. 1B), these molecules may or may not share the same binding site
331 or manifest similar binding mode to the same site on ASIC3. To address this
332 aspect, we performed *in silico* blind docking experiments with GMQ and GBZ
333 against our rASIC3 homology model [48]. In this unbiased docking approach,
334 GMQ preferentially docked to a pocket located in the palm domain of rASIC3
335 (Fig.3E) which has been computationally and experimentally established in
336 previous studies as the likely binding site for GMQ and designated as the
337 nonproton ligand sensor domain [21,50]. In our hands, the guanidinium moiety of
338 GMQ seems to form two salt bridges with E423 whilst the 4-methylquinazoline
339 moiety makes a hydrophobic interaction with L77 and V425 (Fig. 3F).
340 Interestingly, GBZ also docked to the same location (Fig. 3E). Whilst similar salt
341 bridges are also retained in the best docked pose of GBZ, no comparable
342 hydrophobic interactions were discernible with L77 and V425, presumably due to
343 lack of an additional aromatic ring when compared to GMQ structure (Fig.3F).
344
345 Taken together, these results indicate that GBZ modulates rASIC3 in the mild
346 acidic range and that its binding site likely overlaps with that of GMQ, the so called
347 nonproton ligand sensor domain. However, their precise modes of binding may
348 be different, which may underlie the different potencies observed on rASIC3
349 current activation.
350

351 **The GBZ derivative, sephin1, positively modulates rASIC3**

352 Recently, it has been demonstrated that a GBZ derivative without α2-
353 adrenoceptor activity, sephin1 (also known as IFB-088; Fig.4A) acts as an
354 inhibitor of a regulatory subunit of the stress-induced protein phosphatase 1
355 (PPP1R15A) [51]. Sephin1 is effectively the mono-chlorinated version of GBZ
356 and is currently under investigation in clinical trials and hence was not included
357 in the eDrug3D database that we initially screened with ROCS using GMQ as
358 bait. ROCS-based alignment of sephin1 with GMQ revealed by far the highest
359 similarity among the 5 initially selected FDA-approved compounds in terms of
360 both 3D shape (>90%) and chemical features (>50%) with an overall TC score of

361 1.481 (Fig. 4A). In agreement with this, sephin1 appeared to be the most similar
362 to GMQ among all FDA-approved selected drugs in terms of the molecular field
363 points with the highest overall field score (Field Score = 0.847, Fig. 4B).
364
365 Given the high molecular similarity observed *in silico* for sephin1 and GMQ/GBZ,
366 we evaluated the effect of sephin1 on the acid-induced rASIC3 response. Firstly,
367 we observed that sephin1 (500 μM) did not affect the transient component of pH
368 6-induced rASIC3 activation, but it did induce an increase in the amplitude of the
369 sustained component (I_{peak} pH 6: 782.8 ± 98.5 pA/pF vs I_{peak} pH 6 + sephin1:
370 775.1 ± 108.7 pA/pF, paired t-test, n = 10, p = 0.82; I_{5s} pH 6: 4.3 ± 0.6 pA/pF vs
371 I_{5s} pH 6 + sephin1: 11.2 ± 2.8 pA/pF, paired t-test, n = 10, p = 0.03, Fig. 4B and
372 4C) without significantly affecting the I_{5s}/I_{peak} ratio (I_{5s}/I_{peak} pH 6: 0.3 ± 0.1 pA/pF
373 vs I_{5s}/I_{peak} pH 6 + sephin1: 0.6 ± 0.2 pA/pF, paired t-test, n = 10, p = 0.13) or the
374 inactivation time constant (Tau: 301.4 ± 16.5 ms vs 336.9 ± 34.4 ms, paired t-
375 test, n = 10, p = 0.09, Fig. 4C) . Similarly to GMQ and GBZ, both 500 μM and 1
376 mM sephin1 also activated rASIC3 at neutral pH (Fig. 4C and 4E insets) with an
377 EC_{50} of a similar magnitude to that described for GMQ (GMQ = 0.68 mM [21] vs.
378 sephin1 = 0.35 mM) (Fig. 4F). Furthermore, like GMQ and GBZ, sephin1 induced
379 a strong sensitisation, in a dose-dependent fashion, of the transient and
380 sustained components of the pH 7-induced rASIC3 activation (Fig. 5A-D),
381 revealing an EC_{50} of 28.93 μM for the rASIC3 transient current at pH 7 (Fig. 5B).
382 Given the high similarities in the action of sephin1 and GMQ, we hypothesized
383 that sephin1 also binds to the nonproton ligand sensor domain of rASIC3.
384 Similarly to GBZ, *in silico* blind docking experiments showed the likely interaction
385 of sephin1 with the E423 of the nonproton ligand sensor domain, but not E79,
386 together with possible hydrophobic interaction of the aromatic ring of sephin1 with
387 residue A378 (Fig. 5E and 5F). We next tested the pH dependency of rASIC3
388 modulation by sephin1. The application of different pH solutions ranging from pH
389 7.4 to 5 (Fig. 5G and 5H) on rASIC3 induced currents of increasing magnitude to
390 produce a sigmoidal curve that could be fitted to reveal a pH_{50} value of 6.36 (Fig.
391 5G inset), in accordance with previous reports [7,52]. However, in the presence
392 of sephin1 (500 μM), rASIC3 transient activation followed a pH-dependent,
393 biphasic curve (Fig. 5H inset), suggesting an interplay between the action of
394 sephin1 on rASIC3 and its proton activation. As showed previously by Yu et al.

395 using GMQ [21], sephin1 activated rASIC3 at neutral pH, but also potentiated its
396 sustained current at all pH solutions tested, showing a Gaussian distribution with
397 a peak at pH 6.56 (r^2 = 0.43, Fig. 5I). Altogether, these results show that sephin1
398 modulates rASIC3 activation possibly through interacting with the nonproton
399 ligand sensor domain of the channel.

400 # Discussion

401 The ASIC family of ion channels have been implicated in many physiological and
402 pathological processes including nociception [53–55], where they have been
403 established as attractive pharmacological targets for treating pain. ASIC3 is
404 considered of particular interest given its high expression in primary sensory
405 neurones [10] and its involvement in inflammatory pain originating from different
406 tissues including muscle, joints and skin [26–28,56–58]. Therefore, the
407 exploration of novel ASIC3 modulators could increase our knowledge of ion
408 channel function and also be pivotal for the development of new strategies to
409 counteract the detrimental effects of dysregulated ASIC3 activity in
410 pathophysiological states. Many molecules that modulate ASIC3 function have
411 been discovered, ranging from non-selective ASIC3 blockers such as amiloride
412 that acts as a pore blocker and paradoxically stimulates ASIC3 at neutral pH [3],
413 to more specific molecules, such as the inhibitory toxin APETx2, which inhibits
414 the acid-induced transient ASIC3 current [25], and the selective agonist GMQ,
415 which activates ASIC3 at neutral pH and potentiates its activation in response to
416 an acidic stimulus through the nonproton ligand sensor domain of ASIC3 [21,61].
417 In the present study, we used a ligand-based *in silico* screening of FDA-approved
418 drugs to identify novel rASIC3 modulators. Of the top 150 hits ranked by TC
419 score, we selected 5 different drugs with the highest structural and chemical
420 resemblance to GMQ (Fig. 1A), including the presence of a guanidine group.
421 Using an independent algorithm implemented in Cresset's Forge™, we then
422 aligned these 5 drugs with GMQ and compared their surface electrostatic
423 properties represented by the molecular field points. Of the selected drugs, GBZ
424 showed a striking resemblance to GMQ with regard to surface electrostatics and
425 this was reflected in the highest observed value for the field score (0.80). Of the
426 remaining 4 drugs, only BRI which had the 2nd best field score, showed some
427 degree of electrostatic similarity with GMQ (Fig.1B).
428
429 We next sought to experimentally evaluate the effects of these drugs on acid-
430 induced rASIC3 activation. Only one of the drugs tested showed a modulatory
431 effect on rASIC3 acid response to pH 6, namely GBZ, an α2-adrenoceptor
432 agonist. When compared to GMQ, GBZ exhibited a high TC score (1.086) (Fig.

433 1B) and the highest molecular field score (0.8) among the FDA-approved drugs
434 selected (Fig. 1), together with the presence of an explicit guanidine group.
435 Interestingly, TIZ and BRI that showed a higher TC score (Fig. 1A; 1.047 and
436 1.161, respectively) than GBZ and a lower field score in terms of surface
437 electrostatics but the presence of an implicit guanidine moiety (Fig. 1B), did not
438 modulate rASIC3 function, suggesting that a combination of structural and
439 chemical similarities with GMQ and the presence of an explicit guanidine group
440 are required to modulate ASIC3. Nevertheless, it was perhaps unsurprising to
441 observe that GBZ followed a similar mode of action to GMQ, being capable of
442 activating rASIC3 at neutral pH (Fig. 2A and 3A) and inducing a non-desensitising
443 inward current, however its potency was lower than that described for GMQ.
444 Based on our findings from the blind docking experiments against the rASIC3
445 homology model (Fig. 3E), this difference could be explained by the lack of
446 interaction with the core residue L77 and the adjacent residue V425. Such
447 interactions are observed for GMQ in our docking experiment (Fig. 3F) and have
448 been previously shown to be important in the interaction of the 4-
449 methylquinazoline moiety of GMQ [61].This is plausible because, unlike GMQ,
450 GBZ lacks a second aromatic moiety in an appropriate position to allow such
451 hydrophobic contacts. Moreover, the sensitisation of the pH 6-induced rASIC3
452 activation observed by GBZ (Fig. 2A and 2B) suggests a more pronounced effect
453 of the drug in channel opening and desensitisation in response to low acidic
454 stimulus, contrary to the more dominant effect of protons in the GMQ sensitisation
455 at lower pH [21].
456
457 GBZ is an orally active α2-adrenoceptor agonist that has been used for many
458 years as an antihypertensive drug [62]. However, GBZ also binds to the
459 regulatory subunit of protein phosphatase 1, PPP1R15A, disrupting the stress-
460 induced dephosphorylation of the α subunit of the translation initiation factor 2
461 (eIF2α), which protects against the detrimental accumulation of misfolded
462 proteins in the endoplasmic reticulum (ER) [63] and has been proven effective in
463 animal models that mimic misfolding protein diseases such as multiple sclerosis
464 [64]. A recent study has identified a mono-chlorinated version of GBZ, sephin1,
465 which retains the GBZ PPP1R15A inhibition activity, but without adrenoceptor
466 activity [51] and it has also been shown to be effective in animal models of

467 amyotrophic lateral sclerosis [51], Charcot-Marie-Tooth 1B (CMT1B) neuropathy
468 [51] and multiple sclerosis [39]. Given the efficacy of sephin1 to ameliorate the
469 pathogenesis of misfolding protein diseases, InFlectis Bioscience has begun the
470 Phase I clinical trials to evaluate the safety of sephin1 (IFB-088) with the aim of
471 evaluating its effect on the treatment of Charcot-Marie-Tooth 1B (CMT1B)
472 disorder.
473
474 As a result of the similar pharmacological profile of GBZ to GMQ and with the
475 intention of identifying a more selective rASIC3 modulator without adrenoceptor
476 activity, we tested the effect of sephin1 on acid-induced rASIC3 activation. We
477 observed that sephin1 shared a similar pharmacological profile with GBZ and
478 GMQ, sensitising the response (sustained component) of rASIC3 to low pH (pH
479 6) (Fig. 4C and 4D) and mild acidosis (pH 7) (Fig. 5A-D), and activating rASIC3
480 at neutral pH (Fig.4E). These results were consistent with our expectations given
481 that sephin1 appeared to be most similar to GMQ in terms of structural and
482 chemical properties, exhibiting the highest TC score (Fig. 4A), and in terms of
483 molecular field points with the highest overall field score (Fig. 4B). Moreover,
484 increasing concentrations of sephin1 induced increasing potentiation of the pH 7-
485 induced rASIC3 activation (Fig. 5A). Our docking experiments indicated that
486 sephin1 is likely to bind to the nonproton ligand sensor domain and, as we
487 observed for GMQ and GBZ, the negatively charged residue E423 is likely to
488 interact with the explicit guanidinium group of sephin1 (Fig. 5E and 5F). However,
489 compared to GBZ, sephin1's lack of a chloride atom in the aromatic ring seems
490 to allow it to make hydrophobic interactions with surrounding residues like A378,
491 but not with L77 and Val425 as observed for GMQ (Fig.3F). Overall, these
492 interactions likely underlie differential recognition of sephin1 at the nonproton
493 ligand sensor domain of ASIC3, compared to that of GMQ and GBZ.
494
495 Sephin1 is able to selectively disrupt the PPP1R15A-PP1c complex at 50 μM in
496 cells *in vitro* and after oral administration, sephin1 accumulates in the nervous
497 system reaching concentrations of up to 1 μM in the brain and sciatic nerve [51].
498 Moreover, a 2-week treatment with sephin1 at 100 nM has shown efficacy in
499 rescuing myelination of the dorsal root ganglia in a mouse model that mimics
500 Charcot-Marie-Tooth 1B (CMT1B) in humans. Given the high functional

501 expression of rASIC3 in DRG neurones and its involvement in pain derived from
502 inflammatory diseases, together with the action of sephin1 observed on the
503 channel, it is possible that sephin1 treatment could induce and/or exacerbate pain
504 due to the activation of ASIC3 in DRG neurones, however our results show that
505 both activation of rASIC3 at neutral pH and potentiation of the response to mild
506 acidosis (pH 7) require higher concentrations of sephin1 (Fig. 4F and 5A) than
507 those observed to be beneficial in treating misfolding protein diseases in mice.
508 However, the possible additive effects of ASIC3 activated by sephin1 and other
509 endogenous molecules found in the inflammatory soup such as arachidonic acid,
510 which also potentiates acid-induced response of ASIC3 [17] cannot be excluded.
511 Moreover, ASICs function as trimers, displaying different pharmacological
512 profiles depending upon subunit composition. In the present study, we have not
513 evaluated the effect of sephin1 in heteromeric ASIC3-containing channels or
514 other homomeric ASIC channels, and therefore, we cannot hypothesise what
515 might be the potential effects of sephin1 *in vivo*. For instance, GMQ modulates
516 ASIC1a and ASIC1b by shifting their pH dependence of activation to more acidic
517 values [60], precisely the opposite effect seen for ASIC3, effect attributed to
518 structural differences in the extracellular domain of ASIC1a/b and ASIC3 [65].
519 Given the pharmacological and structural resemblance of sephin1 to GMQ, it is
520 possible that sephin1 induces similar modulatory effects on other ASIC subunits.
521 Nevertheless, we believe that the evaluation of pain thresholds in mice and
522 humans used to study the effect of sephin1 in misfolding protein disease should
523 be considered in future studies.
524
525 In summary, we have identified new rASIC3 modulators using a ligand-based *in*
526 *silico* approach, namely GBZ and sephin1, and evaluated their effect on rASIC3
527 function using electrophysiology. Here we provide proof of principle, using a size-
528 restricted chemical library (i.e. FDA-approved drug library), but believe this
529 approach can be exploited in the future to screen much larger chemical space,
530 enabling the identification of novel chemical scaffolds that act as ASIC
531 modulators.

Acknowledgements

The authors declare no competing financial interests. This work was supported by Versus Arthritis Research Grants (RG20930 and RG21973; GC and EStJS), BBSRC grant (BB/R006210/1; JRFH and EStJS), BBSRC-funded studentships (LAP and JCG, BB/M011194/1) and Gates Cambridge Trust (SC). TR gratefully acknowledges OpenEye Scientific Software and Cresset for granting academic licenses for some software used in the present study.

Author Contributions

GC designed the research, conducted the experiments, acquired and analysed the data and wrote the manuscript. LAP, JCG, SC, EA and JRFH acquired and analysed the data. TR and EStJS designed the research and wrote the manuscript. All authors approved the final version of the manuscript.

Declaration of Conflicting Interests

The authors have no conflicting interests to declare.

548 # References

549

550 [1] L.A. Pattison, G. Callejo, E. St John Smith, Evolution of acid nociception:
551 ion channels and receptors for detecting acid, Philos. Trans. R. Soc. B. In
552 press (2019).

553 [2] S. Kellenberger, L. Schild, International Union of Basic and Clinical
554 Pharmacology. XCI. Structure, Function, and Pharmacology of Acid-
555 Sensing Ion Channels and the Epithelial Na+ Channel., Pharmacol. Rev.
556 67 (2015) 1–35. doi:10.1124/pr.114.009225.

557 [3] R. Waldmann, G. Champigny, F. Bassilana, C. Heurteaux, M. Lazdunski,
558 A proton-gated cation channel involved in acid-sensing, Nature. 386 (1997)
559 173–177.

560 [4] S. Gründer, M. Pusch, Biophysical properties of acid-sensing ion channels
561 (ASICs), Neuropharmacology. 94 (2015) 9–18.
562 doi:10.1016/j.neuropharm.2014.12.016.

563 [5] E. Deval, E. Lingueglia, Acid-Sensing Ion Channels and nociception in the
564 peripheral and central nervous systems, Neuropharmacology. 94 (2015)
565 49–57. doi:10.1016/j.neuropharm.2015.02.009.

566 [6] S. Gründer, M. Pusch, Neuropharmacology Biophysical properties of acid-
567 sensing ion channels (ASICs), Neuropharmacology. (2015) 1–10.
568 doi:10.1016/j.neuropharm.2014.12.016.

569 [7] M. Hesselager, pH Dependency and Desensitization Kinetics of
570 Heterologously Expressed Combinations of Acid-sensing Ion Channel
571 Subunits, J. Biol. Chem. 279 (2004) 11006–11015.

572 [8] J. Jasti, H. Furukawa, E.B. Gonzales, E. Gouaux, Structure of acid-sensing
573 ion channel 1 at 1.9 A resolution and low pH., Nature. 449 (2007) 316–23.
574 doi:10.1038/nature06163.

575 [9] L.-N. Schuhmacher, G. Callejo, S. Srivats, E.S.J. Smith, Naked mole-rat
576 acid-sensing ion channel 3 forms nonfunctional homomers, but functional
577 heteromers, J. Biol. Chem. 1 (2017) jbc.M117.807859.
578 doi:10.1074/jbc.M117.807859.

579 [10] L.-N. Schuhmacher, E.S.J. Smith, Expression of acid-sensing ion channels
580 and selection of reference genes in mouse and naked mole rat, Mol. Brain.
581 9 (2016) 97. doi:10.1186/s13041-016-0279-2.

582 [11] E. Boscardin, O. Alijevic, E. Hummler, S. Frateschi, S. Kellenberger, The
583 function and regulation of acid-sensing ion channels (ASICs) and the
584 epithelial Na+channel (ENaC): IUPHAR Review 19, Br. J. Pharmacol.
585 (2016) 2671–2701. doi:10.1111/bph.13533.
586 [12] D. Omerbašić, L.-N. Schuhmacher, Y.-A. Bernal Sierra, E.S.J. Smith, G.R.
587 Lewin, ASICs and mammalian mechanoreceptor function.,
588 Neuropharmacology. (2014) 1–7. doi:10.1016/j.neuropharm.2014.12.007.
589 [13] G. Callejo, A. Castellanos, M. Castany, A. Gual, C. Luna, M.C. Acosta, J.
590 Gallar, J.P. Giblin, X. Gasull, Acid-sensing ion channels detect moderate
591 acidifications to induce ocular pain, Pain. 156 (2015) 483–495.
592 doi:10.1097/01.j.pain.0000460335.49525.17.
593 [14] A. Baron, E. Lingueglia, Pharmacology of acid-sensing ion channels -
594 Physiological and therapeutical perspectives., Neuropharmacology. (2015)
595 1–17. doi:10.1016/j.neuropharm.2015.01.005.
596 [15] R. Waldmann, F. Bassilana, J. de Weille, G. Champigny, C. Heurteaux, M.
597 Lazdunski, Molecular Cloning of a Non-inactivating Proton-gated Na+
598 Channel Specific for Sensory Neurons, J. Biol. Chem. 272 (1997) 20975–
599 20978. doi:10.1074/jbc.272.34.20975.
600 [16] J. Yagi, H.N. Wenk, L. a Naves, E.W. McCleskey, Sustained currents
601 through ASIC3 ion channels at the modest pH changes that occur during
602 myocardial ischemia., Circ. Res. 99 (2006) 501–9.
603 doi:10.1161/01.RES.0000238388.79295.4c.
604 [17] E.S. Smith, H. Cadiou, P. a. McNaughton, Arachidonic acid potentiates
605 acid-sensing ion channels in rat sensory neurons by a direct action,
606 Neuroscience. 145 (2007) 686–698.
607 doi:10.1016/j.neuroscience.2006.12.024.
608 [18] X. Wang, W.-G. Li, Y. Yu, X. Xiao, J. Cheng, W.-Z. Zeng, Z. Peng, M. Xi
609 Zhu, T.-L. Xu, Serotonin facilitates peripheral pain sensitivity in a manner
610 that depends on the nonproton ligand sensing domain of ASIC3 channel.,
611 J. Neurosci. 33 (2013) 4265–79. doi:10.1523/JNEUROSCI.3376-12.2013.
612 [19] T.W. Sherwood, C.C. Askwith, Dynorphin opioid peptides enhance acid-
613 sensing ion channel 1a activity and acidosis-induced neuronal death., J.
614 Neurosci. 29 (2009) 14371–80. doi:10.1523/JNEUROSCI.2186-09.2009.
615 [20] D.C. Immke, E.W. McCleskey, Lactate enhances the acid-sensing Na+

616 channel on ischemia-sensing neurons., Nat. Neurosci. 4 (2001) 869–70.
617 doi:10.1038/nn0901-869.
618 [21] Y. Yu, Z. Chen, W.-G. Li, H. Cao, E.-G. Feng, F. Yu, H. Liu, H. Jiang, T.-L.
619 Xu, A nonproton ligand sensor in the acid-sensing ion channel., Neuron. 68
620 (2010) 61–72. doi:10.1016/j.neuron.2010.09.001.
621 [22] W.-G. Li, Y. Yu, Z.-D. Zhang, H. Cao, T.-L. Xu, ASIC3 channels integrate
622 agmatine and multiple inflammatory signals through the nonproton ligand
623 sensing domain., Mol. Pain. 6 (2010) 88. doi:10.1186/1744-8069-6-88.
624 [23] S. Marra, R. Ferru-clément, V. Breuil, A. Delaunay, M. Christin, V. Friend,
625 S. Sebille, C. Cognard, T. Ferreira, C. Roux, L. Euller-ziegler, J. Noel, E.
626 Lingueglia, E. Deval, Non-acidic activation of pain-related Acid-Sensing Ion
627 Channel 3 by lipids, EMBO J. 35 (2016) 1–15.
628 doi:10.15252/embj.201592335.
629 [24] B. Cristofori-Armstrong, L.D. Rash, Acid-sensing ion channel (ASIC)
630 structure and function: Insights from spider, snake and sea anemone
631 venoms, Neuropharmacology. 127 (2017) 173–184.
632 doi:10.1016/j.neuropharm.2017.04.042.
633 [25] S. Diochot, A. Baron, L.D. Rash, E. Deval, P. Escoubas, S. Scarzello, M.
634 Salinas, M. Lazdunski, A new sea anemone peptide, APETx2, inhibits
635 ASIC3, a major acid-sensitive channel in sensory neurons., EMBO J. 23
636 (2004) 1516–25. doi:10.1038/sj.emboj.7600177.
637 [26] E. Deval, J. Noël, N. Lay, A. Alloui, S. Diochot, V. Friend, M. Jodar, M.
638 Lazdunski, E. Lingueglia, ASIC3, a sensor of acidic and primary
639 inflammatory pain, EMBO J. 27 (2008) 3047–3055.
640 [27] W.S. Hsieh, C.C. Kung, S.L. Huang, S.C. Lin, W.H. Sun, TDAG8, TRPV1,
641 and ASIC3 involved in establishing hyperalgesic priming in experimental
642 rheumatoid arthritis, Sci. Rep. 7 (2017) 1–14. doi:10.1038/s41598-017-
643 09200-6.
644 [28] M. Ikeuchi, S.J. Kolker, L.A. Burnes, R.Y. Walder, K.A. Sluka, Role of
645 ASIC3 in the primary and secondary hyperalgesia produced by joint
646 inflammation in mice., Pain. 137 (2008) 662–9.
647 doi:10.1016/j.pain.2008.01.020.
648 [29] M. Ikeuchi, S.J. Kolker, K.A. Sluka, Acid-sensing ion channel 3 expression
649 in mouse knee joint afferents and effects of carrageenan-induced arthritis.,

650 J. Pain. 10 (2009) 336–42. doi:10.1016/j.jpain.2008.10.010.
651 [30] M. Izumi, M. Ikeuchi, Q. Ji, T. Tani, Local ASIC3 modulates pain and
652 disease progression in a rat model of osteoarthritis., J. Biomed. Sci. 19
653 (2012) 77. doi:10.1186/1423-0127-19-77.
654 [31] R.C.W. Jones, E. Otsuka, E. Wagstrom, C.S. Jensen, M.P. Price, G.F.
655 Gebhart, Short-term sensitization of colon mechanoreceptors is associated
656 with long-term hypersensitivity to colon distention in the mouse.,
657 Gastroenterology. 133 (2007) 184–94. doi:10.1053/j.gastro.2007.04.042.
658 [32] C. Reimers, C.-H. Lee, H. Kalbacher, Y. Tian, C.-H. Hung, A. Schmidt, L.
659 Prokop, S. Kauferstein, D. Mebs, C.-C. Chen, S. Grunder, Identification of
660 a cono-{RFamide} from the venom of {Conus} textile that targets {ASIC}3
661 and enhances muscle pain., Proc. Natl. Acad. Sci. U. S. A. 114 (2017)
662 E3507--E3515. doi:10.1073/pnas.1616232114.
663 [33] K.A. Sluka, R. Radhakrishnan, C.J. Benson, J.O. Eshcol, M.P. Price, K.
664 Babinski, K.M. Audette, D.C. Yeomans, S.P. Wilson, ASIC3 in muscle
665 mediates mechanical, but not heat, hyperalgesia associated with muscle
666 inflammation, Pain. 129 (2007) 102–112.
667 [34] A.A. Staniland, S.B. McMahon, Mice lacking acid-sensing ion channels
668 (ASIC) 1 or 2, but not ASIC3, show increased pain behaviour in the formalin
669 test., Eur. J. Pain. 13 (2009) 554–63. doi:10.1016/j.ejpain.2008.07.001.
670 [35] K. a Sluka, L. a Rasmussen, M.M. Edgar, J.M. O'Donnell, R.Y. Walder, S.J.
671 Kolker, D.L. Boyle, G.S. Firestein, Acid-sensing ion channel 3 deficiency
672 increases inflammation but decreases pain behavior in murine arthritis.,
673 Arthritis Rheum. 65 (2013) 1194–202. doi:10.1002/art.37862.
674 [36] D.J. Scholz, M.A. Janich, U. Kollisch, R.F. Schulte, J.H. Ardenkjaer-Larsen,
675 A. Frank, A. Haase, M. Schwaiger, M.I. Menzel, Quantified pH imaging with
676 hyperpolarized (13) C-bicarbonate., Magn. Reson. Med. 73 (2015) 2274–
677 2282. doi:10.1002/mrm.25357.
678 [37] A.J. Wright, Z.M.A. Husson, D.-E. Hu, G. Callejo, K.M. Brindle, E.S.J.
679 Smith, Increased hyperpolarized [1-(13) C] lactate production in a model of
680 joint inflammation is not accompanied by tissue acidosis as assessed using
681 hyperpolarized (13) C-labelled bicarbonate., NMR Biomed. 31 (2018)
682 e3892. doi:10.1002/nbm.3892.
683 [38] F.S.J. Tennant, R.A. Rawson, Guanabenz acetate: a new, long-acting

684 alpha-two adrenergic agonist for opioid withdrawal., NIDA Res. Monogr. 49
685 (1984) 338–343.
686 [39] Y. Chen, J.R. Podojil, R.B. Kunjamma, J. Jones, M. Weiner, W. Lin, S.D.
687 Miller, B. Popko, Sephin1, which prolongs the integrated stress response,
688 is a promising therapeutic for multiple sclerosis., Brain. 142 (2019) 344–
689 361. doi:10.1093/brain/awy322.
690 [40] N.M. O'Boyle, M. Banck, C.A. James, C. Morley, T. Vandermeersch, G.R.
691 Hutchison, Open {Babel}: {An} open chemical toolbox., J. Cheminform. 3
692 (2011) 33. doi:10.1186/1758-2946-3-33.
693 [41] P.C.D. Hawkins, A.G. Skillman, A. Nicholls, Comparison of shape-
694 matching and docking as virtual screening tools., J. Med. Chem. 50 (2007)
695 74–82. doi:10.1021/jm0603365.
696 [42] E. Pihan, L. Colliandre, J.-F. Guichou, D. Douguet, e-{Drug}3D: 3D
697 structure collections dedicated to drug repurposing and fragment-based
698 drug design., Bioinformatics. 28 (2012) 1540–1541.
699 doi:10.1093/bioinformatics/bts186.
700 [43] P.C.D. Hawkins, A.G. Skillman, G.L. Warren, B.A. Ellingson, M.T. Stahl,
701 Conformer generation with {OMEGA}: algorithm and validation using high
702 quality structures from the {Protein} {Databank} and {Cambridge}
703 {Structural} {Database}., J. Chem. Inf. Model. 50 (2010) 572–584.
704 doi:10.1021/ci100031x.
705 [44] E. Naylor, A. Arredouani, S.R. Vasudevan, A.M. Lewis, R. Parkesh, A.
706 Mizote, D. Rosen, J.M. Thomas, M. Izumi, A. Ganesan, A. Galione, G.C.
707 Churchill, Identification of a chemical probe for {NAADP} by virtual
708 screening., Nat. Chem. Biol. 5 (2009) 220–226. doi:10.1038/nchembio.150.
709 [45] T. Cheeseright, M. Mackey, S. Rose, A. Vinter, Molecular field extrema as
710 descriptors of biological activity: definition and validation., J. Chem. Inf.
711 Model. 46 (2006) 665–676. doi:10.1021/ci050357s.
712 [46] E.S.J. Smith, X. Zhang, H. Cadiou, P.A. McNaughton, Proton binding sites
713 involved in the activation of acid-sensing ion channel ASIC2a, Neurosci.
714 Lett. 426 (2007) 12–17.
715 [47] I. Dittert, J. Benedikt, L. Vyklický, K. Zimmermann, P.W. Reeh, V. Vlachová,
716 Improved superfusion technique for rapid cooling or heating of cultured
717 cells under patch-clamp conditions, J. Neurosci. Methods. 151 (2006) 178–

718 185. doi:10.1016/j.jneumeth.2005.07.005.
719 [48] T. Rahman, E.S.J. Smith, In silico assessment of interaction of sea
720 anemone toxin APETx2 and acid sensing ion channel 3., Biochem.
721 Biophys. Res. Commun. 450 (2014) 384–9.
722 doi:10.1016/j.bbrc.2014.05.130.
723 [49] G.M. Morris, R. Huey, W. Lindstrom, M.F. Sanner, R.K. Belew, D.S.
724 Goodsell, A.J. Olson, {AutoDock}4 and {AutoDockTools}4: {Automated}
725 docking with selective receptor flexibility., J. Comput. Chem. 30 (2009)
726 2785–2791. doi:10.1002/jcc.21256.
727 [50] Y. Yu, W.-G. Li, Z. Chen, H. Cao, H. Yang, H. Jiang, T.-L. Xu, Atomic level
728 characterization of the nonproton ligand-sensing domain of ASIC3
729 channels., J. Biol. Chem. 286 (2011) 24996–5006.
730 doi:10.1074/jbc.M111.239558.
731 [51] I. Das, A. Krzyzosiak, K. Schneider, L. Wrabetz, M. D'Antonio, N. Barry, A.
732 Sigurdardottir, A. Bertolotti, Preventing proteostasis diseases by selective
733 inhibition of a phosphatase regulatory subunit, Science (80-.). 348 (2015)
734 239–242. doi:10.1126/science.aaa4484.
735 [52] L.-N. Schuhmacher, G. Callejo, S. Srivats, E.S.J. Smith, Naked mole-rat
736 acid-sensing ion channel 3 forms nonfunctional homomers, but functional
737 heteromers., J. Biol. Chem. 293 (2018) 1756–1766.
738 doi:10.1074/jbc.M117.807859.
739 [53] E. Deval, J. Noël, X. Gasull, A. Delaunay, A. Alloui, V. Friend, A. Eschalier,
740 M. Lazdunski, E. Lingueglia, Acid-sensing ion channels in postoperative
741 pain, J. Neurosci. 31 (2011) 6059–6066.
742 [54] J.-H. Lin, C.-H. Hung, D.-S. Han, S.-T. Chen, C.-H. Lee, W.-Z. Sun, C.-C.
743 Chen, Sensing acidosis: nociception or sngception?, J. Biomed. Sci. 25
744 (2018) 85. doi:10.1186/s12929-018-0486-5.
745 [55] M. Mazzuca, C. Heurteaux, A. Alloui, S. Diochot, A. Baron, N. Voilley, N.
746 Blondeau, P. Escoubas, A. Gélot, A. Cupo, A. Zimmer, A.M. Zimmer, A.
747 Eschalier, M. Lazdunski, A tarantula peptide against pain via ASIC1a
748 channels and opioid mechanisms, Nat. Neurosci. 10 (2007) 943–945.
749 [56] C.-C. Chen, A. Zimmer, W.-H. Sun, J. Hall, M.J. Brownstein, A. Zimmer, A
750 role for ASIC3 in the modulation of high-intensity pain stimuli., Proc. Natl.
751 Acad. Sci. U. S. A. 99 (2002) 8992–7. doi:10.1073/pnas.122245999.

752 [57] W.-N. Chen, C.-C. Chen, Acid mediates a prolonged antinociception via
753 substance P signaling in acid-induced chronic widespread pain., Mol. Pain.
754 10 (2014) 30. doi:10.1186/1744-8069-10-30.
755 [58] J. Karczewski, R.H. Spencer, V.M. Garsky, A. Liang, M.D. Leitl, M.J. Cato,
756 S.P. Cook, S. Kane, M.O. Urban, Reversal of acid-induced and
757 inflammatory pain by the selective ASIC3 inhibitor, APETx2., Br. J.
758 Pharmacol. 161 (2010) 950–60. doi:10.1111/j.1476-5381.2010.00918.x.
759 [59] W.-G. Li, Y. Yu, C. Huang, H. Cao, T.-L. Xu, The nonproton ligand sensing
760 domain is required for paradoxical stimulation of ASIC3 channels by
761 amiloride, J. Biol. Chem. (2011).
762 [60] O. Alijevic, S. Kellenberger, Subtype-specific modulation of acid-sensing
763 ion channel (ASIC) function by 2-guanidine-4-methylquinazoline., J. Biol.
764 Chem. 287 (2012) 36059–70. doi:10.1074/jbc.M112.360487.
765 [61] Y. Yu, W.-G. Li, Z. Chen, H. Cao, H. Yang, H. Jiang, T.-L. Xu, Atomic level
766 characterization of the nonproton ligand-sensing domain of ASIC3
767 channels., J. Biol. Chem. 286 (2011) 24996–5006.
768 doi:10.1074/jbc.M111.239558.
769 [62] B. Holmes, R.N. Brogden, R.C. Heel, T.M. Speight, G.S. Avery,
770 Guanabenz. {A} review of its pharmacodynamic properties and therapeutic
771 efficacy in hypertension., Drugs. 26 (1983) 212–229.
772 [63] P. Tsaytler, H.P. Harding, D. Ron, A. Bertolotti, Selective inhibition of a
773 regulatory subunit of protein phosphatase 1 restores proteostasis, Science
774 (80-.). 332 (2011) 91–94. doi:10.1126/science.1201396.
775 [64] S.W. Way, J.R. Podojil, B.L. Clayton, A. Zaremba, T.L. Collins, R.B.
776 Kunjamma, A.P. Robinson, P. Brugarolas, R.H. Miller, S.D. Miller, B.
777 Popko, Pharmaceutical integrated stress response enhancement protects
778 oligodendrocytes and provides a potential multiple sclerosis therapeutic.,
779 Nat. Commun. 6 (2015) 6532. doi:10.1038/ncomms7532.
780 [65] T. Besson, E. Lingueglia, M. Salinas, Pharmacological modulation of Acid-
781 Sensing Ion Channels 1a and 3 by amiloride and 2-guanidine-4-
782 methylquinazoline (GMQ), Neuropharmacology. 125 (2017) 429–440.
783 doi:10.1016/j.neuropharm.2017.08.004.
784

785 **Table 1**

786

	I_{Peak} (pA/pF)		I_{5s} (pA/pF)		I_{5s}/I_{Peak} (%)		Tau (ms)	
	Baseline	**Compound effect**	**Baseline**	**Compound effect**	**Baseline**	**Compound effect**	**Baseline**	**Compound effect**
APETx2 (n = 10)	895.55 ± 160.39	301.01 ± 48.83**	5.76 ± 1.17	3.52 ± 0.77*	0.92 ± 0.34	1.53 ± 0.54*	303.12 ± 14.55	243.82 ± 10.06***
GMQ (n = 8)	747.04 ± 107.29	746.18 ± 118.3	2.74 ± 0.36	2.9 ± 0.29	0.40 ± 0.06	0.47 ± 0.09	307.2 ± 16.01	307.36 ± 23.19
Tizanidine (n = 10)	806.1 ± 44.39	866.66 ± 68.76	8.65 ± 1.19	9.25 ± 1.2	1.09 ± 0.14	1.14 ± 0.2	311.15 ± 15.68	318.14 ± 18.60
Guanfacine (n = 10)	1110.47 ± 90.16	1040.74 ± 119.5	7.68 ± 1.27	8.19 ± 1.06	0.68 ± 0.09	0.85 ± 0.14	318.97 ± 21.26	349.97 ± 25.79
Brimonidine (n = 7)	1044.28 ± 102.4	1023.4 ± 144.2	9.4 ± 2.1	8.38 ± 1.85	1.03 ± 0.3	0.93 ± 0.25	290.49 ± 19.13	304.18 ± 31.09
Cycloguanil (n = 11)	1035.98 ± 94.33	1055.7 ± 122.5	15.32 ± 5.77	15.09 ± 5.3	1.27 ± 0.35	1.22 ± 0.28	319.34 ± 8.47	326.95 ± 10.56
Guanabenz (n = 11)	681.83 ± 78.52	773.52 ± 95.37*	9.85 ± 2.32	28.33 ± 6.81*	1.56 ± 0.5	3.92 ± 0.73*	319.45 ± 13.85	415.38 ± 36.55*

787 # Figures/Table Legends

788 **Figure 1. Selected FDA-approved drugs after ligand-based in silico**
789 **screening using GMQ as query molecule.** (A) 2D chemical structure of GMQ
790 and selected FDA-approved drugs (Guanidine or similar moiety is shown in red)
791 and alignment of these drugs with GMQ based on molecular electrostatic field
792 potentials. Forge^{TM} (v 10.4.2; Cresset) was used to align the drug structures with
793 the energy-minimised structure of GMQ. In all cases, the negative, positive and
794 hydrophobic field points are coloured blue, red and gold, respectively (van der
795 Waals isosurfaces are not shown). The sphere size corresponds to possible
796 interaction strength with the cognate probe used for field point calculation. The
797 individual molecular field similarity scores to GMQ (maximum value = 1) are given
798 below right in each panel. (B) Representations of the selected drugs showing
799 similarity in 3D shape and chemical features with GMQ**.** Drugs were chosen from
800 ligand-based in silico screening using ROCS (OpenEye Scientific Software) that
801 ranked them on the basis of Tanimoto Combo Score. The latter is a sum of Shape
802 Tanimoto and Colour Tanimoto score indicating similarity in 3D shape (maximum
803 value = 1) and chemical features (maximum value = 1). The volume of the query
804 molecule (GMQ) is shown as a dotted area and the chemical similarity aspects
805 are shown in different colours. The figure was generated by ROCS Report
806 (OpenEye).
807

808 **Figure 2. Effect of the selected drugs rASIC3 response to pH 6**. (A) Example
809 traces of the effect for the 5 different selected drugs (500 μM) on pH 6-induced
810 rASIC3 activation together with example traces showing the effect of known
811 rASIC3 modulators, APETx2 (1 μM) and GMQ (500 μM). In all cases drugs were
812 applied for 30 s prior to pH 6-induced rASIC3 activation. (B-D) Bar plots showing
813 the effect of the selected drugs, APETx2 and GMQ on transient (peak) (B) and
814 sustained current (C), and inactivation time constant (D) of rASIC3 activation.
815 Values were normalised to baseline pH 6 rASIC3 activation and expressed as
816 means ± SEM (n = 7-11, paired t-test, *p <0.05 and ***p ≤ 0.005 vs baseline pH
817 6 activation).
818

819 **Figure 3. Effect of guanabenz (GBZ) on rASIC3 response to neutral and mild**
820 **acidic pH**. (A) Example traces of rASIC3 activation at neutral pH elicited by GMQ
821 (1 mM) and GBZ (1 mM). Inset showing magnification of GBZ activation. (B) Bar
822 plot showing the quantification of GMQ- and GBZ-induced rASIC3 activation at
823 neutral pH normalised against ASIC3 pH 6 response. Values were normalised
824 against pH 6 rASIC3 activation. (C) Example traces of the effect of GMQ and
825 GBZ potentiation of the pH 7-induced rASIC3 activation. (D) Bar plot showing the
826 quantification of the potentiation induced by GMQ and GBZ of the pH 7-induced
827 rASIC3 activation. Values were normalised against the baseline pH 7 ASCI3
828 activation (n = 6-9, paired t-test, *p ≤ 0.05, **p ≤ 0.01, ****p ≤ 0.001, vs baseline
829 pH 6 activation). (E) The ligand interaction diagrams of GMQ and GBZ were
830 generated using PoseView from their cognate docked complexes (shown in Fig.
831 4F) with rASIC3 model. (F) GMQ and GBZ were blindly docked to a homology
832 model of rASIC3 dimer (green = chain C and pale blue = chain A) using
833 AutoDock4.2.6. Binding poses of the molecules represent the top-ranked docked
834 pose of individual molecules and are shown in (F) global and (F inset) close-up
835 views. GMQ and GBZ are shown in red and cyan stick representations,
836 respectively.
837
838 **Figure 4. Effect of sephin1 on rASIC3 activation.** (A) Comparison of GMQ and
839 sephin1 2D structure and molecular field electrostatics as described in Fig.1 for
840 sephin1 (B) Example trace of effect of sephin1 (500 μM) on pH6-induced rASIC3
841 activation. (B inset) Magnification of rASIC3 activation induced by sephin1 at
842 neutral pH. (C) Bar plot quantifying sephin1 effect on the transient and sustained
843 normalised current and inactivation time constant of the pH 6-induced rASIC3
844 activation expressed as a percentage of the pH 6 baseline activation (n = 10,
845 paired t-test; *p <0.05 vs baseline pH 6 activation). (D) Example trace showing
846 rASIC3 activation by sephin1 at neutral pH. (B inset) Magnification of the current
847 elicited by sephin1 (n = 12). (E) Dose-response effect of increasing
848 concentrations of sephin1 (1 nM–3 mM) applied at neutral pH on rASIC3.
849 Absolute values were normalised using the capacitance of each cell (pA/pF) and
850 expressed as a percentage of the pH 6-induced rASIC3 activation. A non-linear
851 regression using a sigmoidal function was used to determine the EC_{50} of sephin1
852 on rASIC3 (n = 4-12, EC_{50} = 0.68 mM).

853

854 **Fig. 5. Effect of sephin1 on rASIC3 response to mild acidosis (pH 7) and pH-**
855 **dependency**. (A) Dose-response effect of increasing concentrations of sephin1
856 (1μM–1mM) applied at pH 7 on rASIC3. (B) Fitting of normalised values for the
857 transient (peak) and sustained current (pA/pF) obtained in A using a sigmoidal
858 function. (C and D) Bar plot showing the quantification of the data points obtained
859 in A for each sephin1 concentration. Normalised values were expressed as a
860 percentage of the baseline rASIC3 pH 7 activation (n = 8-11, paired t-test, **p ≤
861 0.01, ***p ≤ 0.005, ****p ≤ 0.001, vs baseline pH 7 activation). (E) Ligand
862 interaction diagram of sephin1 generated using PoseView from its cognate
863 docked complex with rASIC3 model. (F) GMQ and sephin1 were blindly docked
864 to a homology model of rASIC3 dimer using AutoDock4.2.6. Binding poses of the
865 molecules represent the top-ranked docked pose of individual molecules and are
866 shown in close-up views. GMQ and sephin1 are shown in red and magenta stick
867 representations, respectively. (G and H) pH-dependent effect of sephin1 on
868 rASIC3. Example traces of rASIC3 response to a pH range from 7.4 to 5 with and
869 without sephin1 (500 μM) (n = 7-11) (G and H insets) pH-response curves of
870 rASIC3 activation by different pH extracellular solutions used with (G inset) and
871 without (H inset) sephin1 (500 μM). (I) Bar plot showing the quantification of the
872 normalised sustained current (pA/pF) elicited by sephin1 at different pH solutions.
873

874 **Table 1. Effect of the selected compounds on rASIC3 current kinetics**.
875 Comparison of the mean ± SEM of the amplitude of the transient (I_{peak}) and
876 sustained (I_{5s}) current, together with the ratio I_{Peak}/I_{5s} and the inactivation time
877 constant (Tau) between baseline rASIC3 responses and after compound
878 application (Paired t-test, *p ≤ 0.05, **p ≤ 0.01, ***p ≤ 0.005).

Figure 1

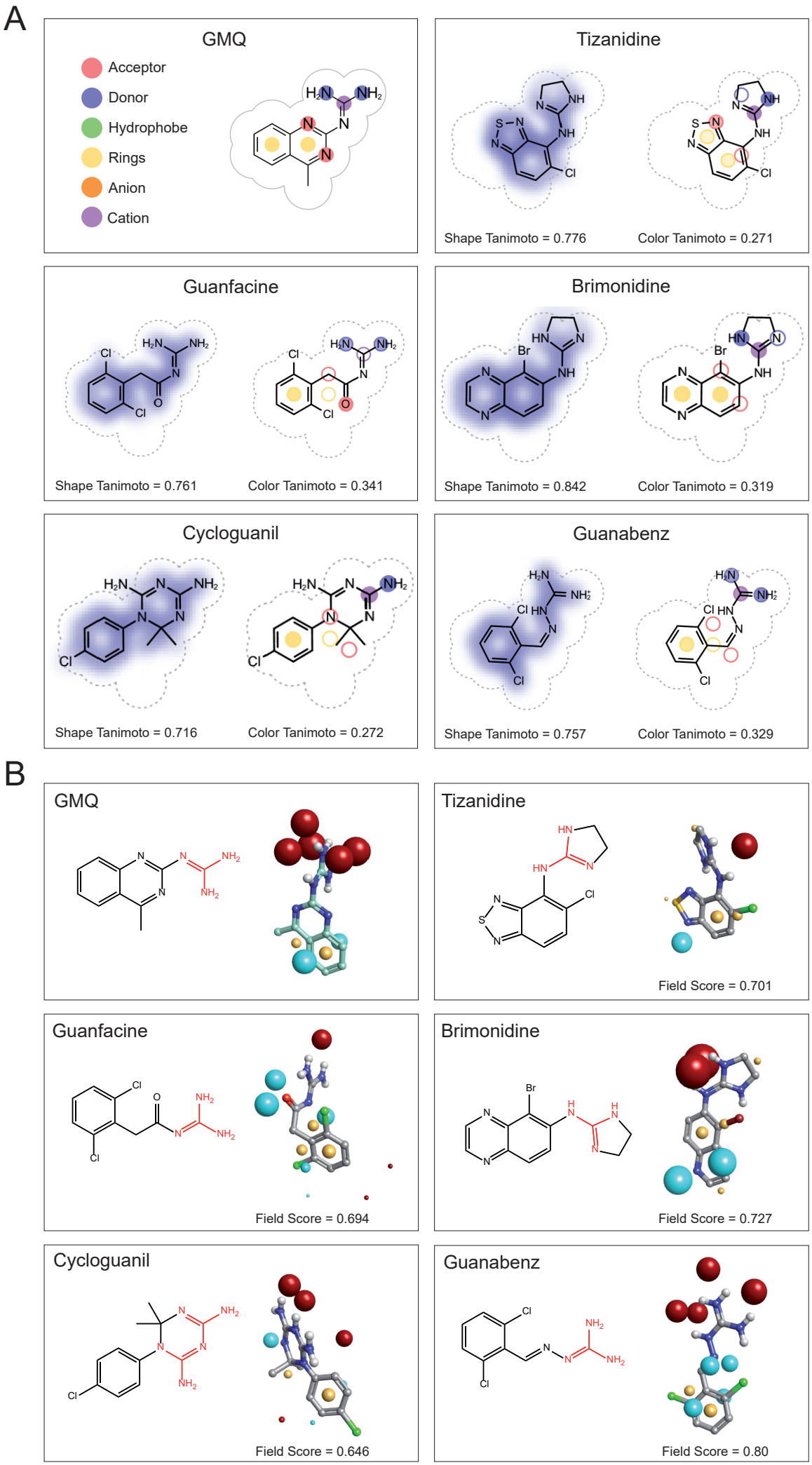
A
GMQ
Acceptor
Donor
Hydrophobe
Rings
Anion
Cation
Tizanidine
Shape Tanimoto = 0.776
Color Tanimoto = 0.271
Guanfacine
Shape Tanimoto = 0.761
Color Tanimoto = 0.341
Brimonidine
Shape Tanimoto = 0.842
Color Tanimoto = 0.319
Cycloguanil
Shape Tanimoto = 0.716
Color Tanimoto = 0.272
Guanabenz
Shape Tanimoto = 0.757
Color Tanimoto = 0.329
B
GMQ
Tizanidine
Field Score = 0.701
Guanfacine
Field Score = 0.694
Brimonidine
Field Score = 0.727
Cycloguanil
Field Score = 0.646
Guanabenz
Field Score = 0.80

Figure 2

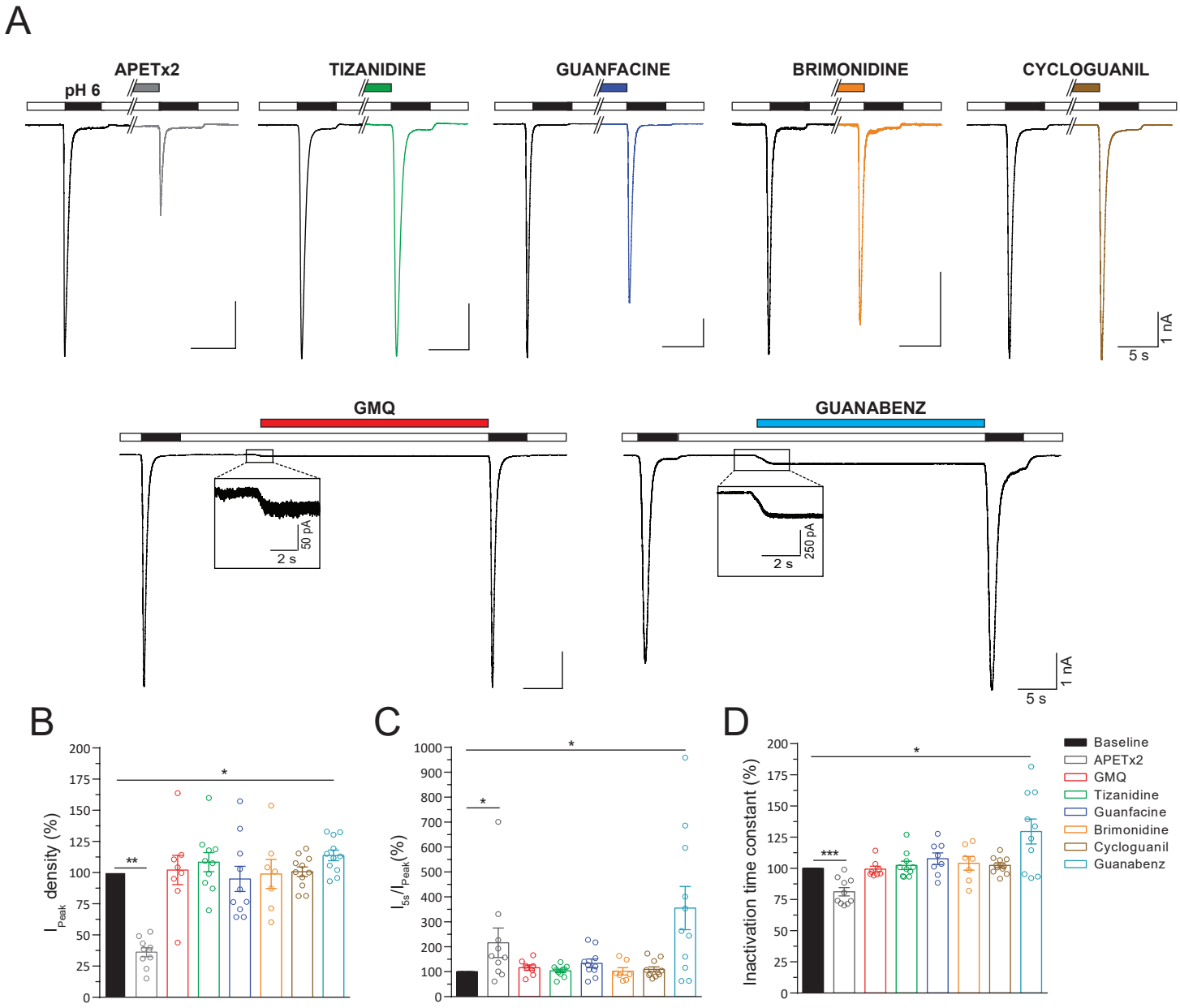
A
APETx2
pH 6
TIZANIDINE
GUANFACINE
BRIMONIDINE
CYCLOGUANIL
1 nA
5 s
GMQ
50 pA
2 s
GUANABENZ
250 pA
2 s
1 nA
5 s
B
I_{Peak} density (%)
C
I_{5s}/I_{Peak}(%)
D
Inactivation time constant (%)
Baseline
APETx2
GMQ
Tizanidine
Guanfacine
Brimonidine
Cycloguanil
Guanabenz

Figure 3

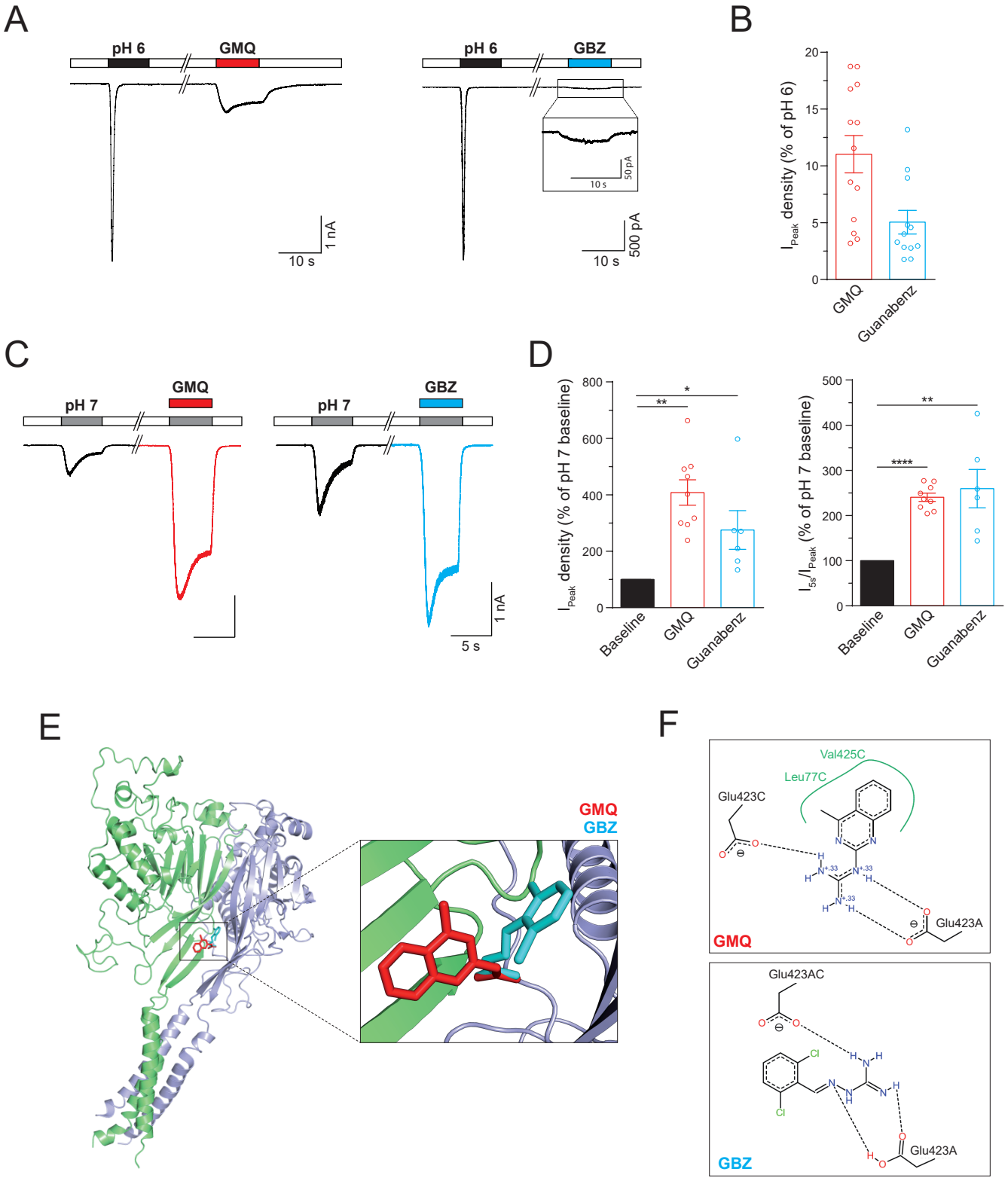
A
pH 6
GMQ
1 nA
10 s
pH 6
GBZ
50 pA
10 s
500 pA
10 s
B
I_{Peak} density (% of pH 6)
GMQ
Guanabenz
C
pH 7
GMQ
pH 7
GBZ
1 nA
5 s
D
I_{Peak} density (% of pH 7 baseline)
Baseline
GMQ
Guanabenz
I_{5s}/I_{Peak} (% of pH 7 baseline)
Baseline
GMQ
Guanabenz
E
GMQ
GBZ
F
Val425C
Leu77C
Glu423C
Glu423A
GMQ
Glu423AC
Glu423A
GBZ

Figure 4

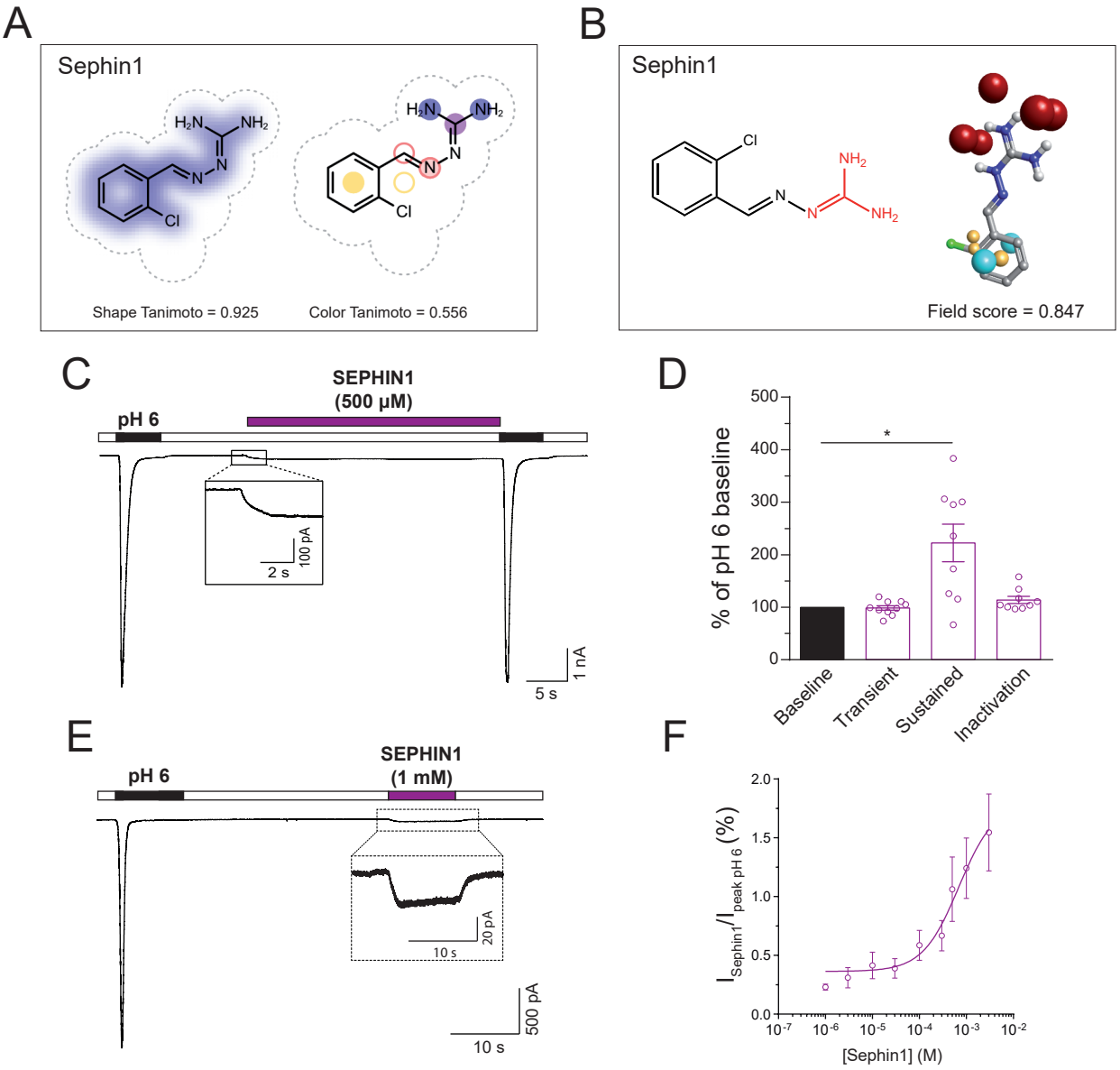
A
Sephin1
Shape Tanimoto = 0.925
Color Tanimoto = 0.556
B
Sephin1
Field score = 0.847
C
SEPHIN1
(500 µM)
pH 6
100 pA
2 s
1 nA
5 s
D
% of pH 6 baseline
Baseline
Transient
Sustained
Inactivation
E
pH 6
SEPHIN1
(1 mM)
20 pA
10 s
500 pA
10 s
F
[Sephin1] (M)

Figure 5

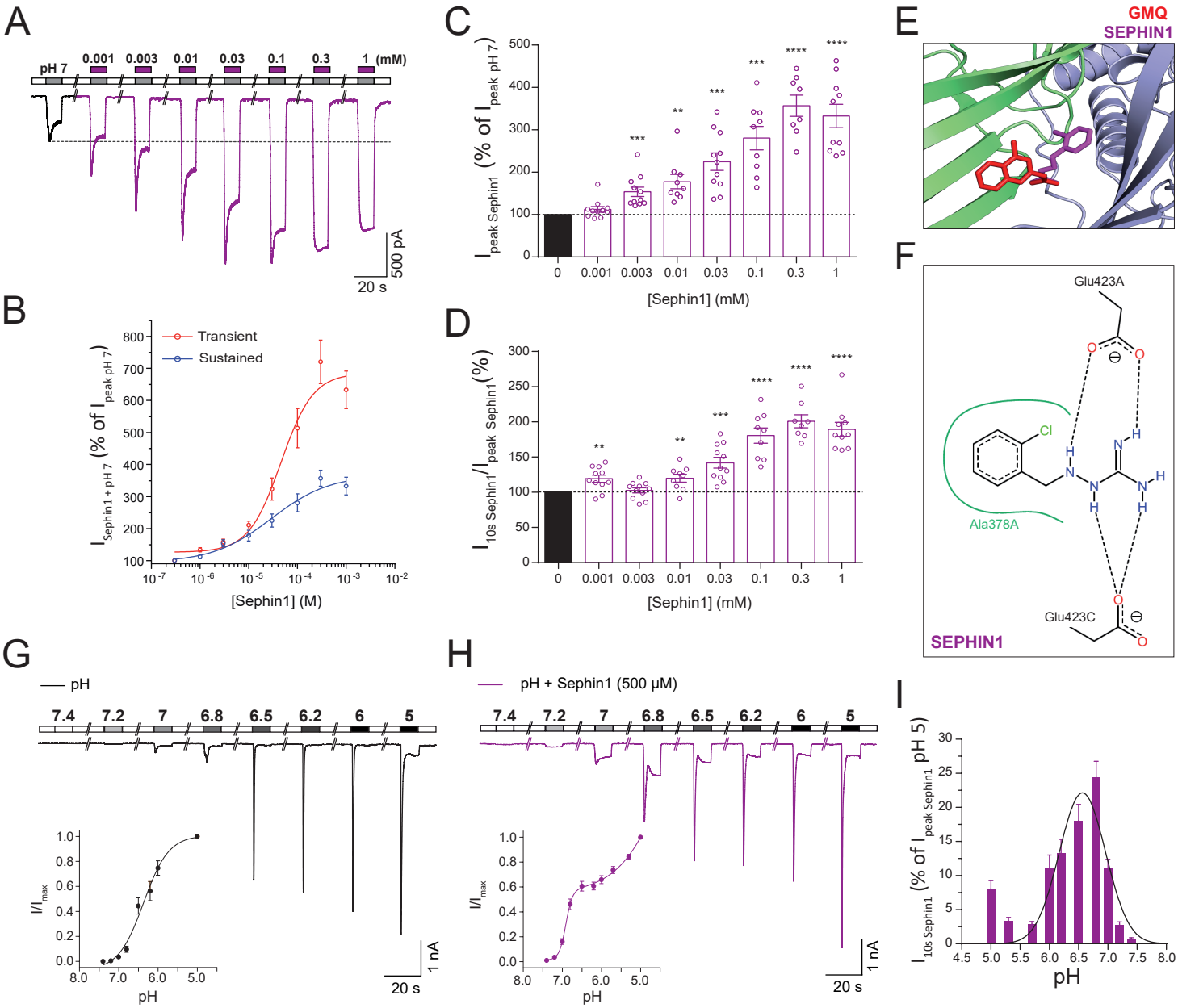
A
pH 7
0.001
0.003
0.01
0.03
0.1
0.3
1 (mM)
500 pA
20 s
B
Transient
Sustained
[Sephin1] (M)
C
[Sephin1] (mM)
D
[Sephin1] (mM)
E
GMQ
SEPHIN1
F
Glu423A
Cl
Ala378A
Glu423C
SEPHIN1
G
pH
7.4
7.2
7
6.8
6.5
6.2
6
5
1 nA
20 s
pH
H
pH + Sephin1 (500 µM)
7.4
7.2
7
6.8
6.5
6.2
6
5
1 nA
20 s
pH
I
pH